Adsorption Behavior of Iron Phthalocyanine on Au(111) Surface at Submonolayer Coverage

Z. H. Cheng, L. Gao, Z. T. Deng, N. Jiang, Q. Liu, D. X. Shi, S. X. Du, H. M. Guo, and H.-J. Gao*

Beijing National Laboratory for Condensed Matter Physics & Institute of Physics, Chinese Academy of Sciences, P.O. Box 603, Beijing 100080, China

Received: January 16, 2007; In Final Form: April 23, 2007

Adsorption behavior of iron(II) phthalocyanine (FePc) on Au(111) surface at submonolayer coverage has been investigated using low-temperature scanning tunneling microscopy (STM) and density functional theory (DFT) calculations. At the initial adsorption stage, FePc molecules prefer to adsorb on terrace dispersedly as isolated adsorbates because of the stronger molecule−substrate interaction than the lateral intermolecular interaction. Two different configurations of FePc on Au(111) surface are resolved on the basis of STM image analysis and are further identified by DFT calculations. When increasing molecule coverage, the intermolecular interaction becomes more important. The FePc molecules assemble to dimers, trimers, and short chains and even peculiar porous hexamers with two configurations. At a saturated coverage, highly ordered FePc monolayer with only one configuration of FePc is observed. The results indicate that the adsorption behavior of FePc on Au(111) is governed by a coverage-dependent competition between molecule−substrate and intermolecular interactions.

Introduction

Organic molecular thin films have attracted much interest in the last few decades because of their potential applications in optical and electronic devices such as organic light-emitting diodes, organic thin-film transistors, and molecular electronic devices in the future.[1−6] Recently, great attention has been focused on the growth of functional molecules on different single-crystalline metal substrates.[7−16] In general, the adsorption and the ordering of molecules on metal surfaces is generally controlled by a subtle balance between the molecule−molecule interaction and molecule−substrate interaction, which is critical for controlling the structure and properties of overlayers.[17−22] The competition between the two interactions is also sensitive to surface coverage, especially in submonolayer region.[23]

Phthalocyanines (Pcs), metal phthalocyanines (MPcs), and their derivatives have attracted special interest of research because of their wide applications in the area of gas-sensing devices, photovoltaic applications, light-emitting diodes, solar and fuel cells, organic field effect transistors, pigments, and dyes.[24−26] Much research on the assembled structure of various MPc has been reported.[16,27−33] However, few investigations of MPc on metal substrate have been carried out at the submonolayer coverage because of the high mobilities of MPc molecules on metal surfaces.[16,34] This prevents a full understanding of fundamental issues, such as the adsorption sites and the interactions between adsorbed MPc molecules. In our previous work,[35] we have studied the epitaxial growth behavior of iron(II) phthalocyanine (FePc) molecules on Au(111) surface at monolayer and multilayer coverages, while the description of molecular adsorption behavior at the submonolayer coverage is very limited.

In this paper, we report the scanning tunneling microscopy (STM) investigation and density functional theory (DFT) calculations on the adsorption configuration and self-assembly behavior of FePc molecules on the Au(111) surface at submonolayer coverages. The results show that the molecules deposited on Au(111) dispersedly at low submonolayer coverage form oligomers and molecular chains at high submonolayer coverage and ordered structures at saturated coverage. It reflects a coverage-dependent competition between molecule−molecule and molecule−substrate interactions. Two different configurations of FePc molecules and a peculiar porous hexamer structure were resolved and identified by a combination of STM and DFT calculations.

Experimental and Calculation Details

The experiments were performed with a low-temperature STM system (LT-STM, Omicron GmbH) equipped in an ultrahigh vacuum (UHV) chamber with a base pressure of 1×10^{-10} mbar. The Au(111) surface was cleaned by repeated Ar ion sputtering and annealing at 700 K until a clean surface was confirmed by STM imaging. FePc (Aldrich, 98+%) was thermally evaporated at 540 K onto Au(111) surface held at room temperature (RT) with molecular beam epitaxy-low energy electron diffraction (MBE-LEED).[13−15] Subsequently, the sample was slowly cooled down to 5 K in the STM chamber. The STM measurements were performed with an electrochemically etched tungsten tip at 5 K. All given voltages are referred to the sample, and the images have been taken in constant-current mode.

In addition to the experimental procedures, DFT calculations were performed. A Perdew−Burke−Ernzerhof (PBE) generalized gradient approximation for the exchange-correlation energy,[36] projector augmented wave (PAW) pseudopotentials,[37,38] and a plane wave basis set implemented in the Vienna ab initio Simulation Package (VASP)[39,40] were used. Because of numerical limitations and the huge size of the system, the surface Brillouin zone was sampled with the Γ point only, and a c(6 × 6) Au(111) supercell with four-layer Au separated by a vacuum layer of 22 Å was used to model the adsorbed system. The cutoff

* To whom correspondence should be addressed. E-mail: hjgao@aphy.iphy.ac.cn.

10.1021/jp070388l CCC: $37.00
Published on Web 06/05/2007

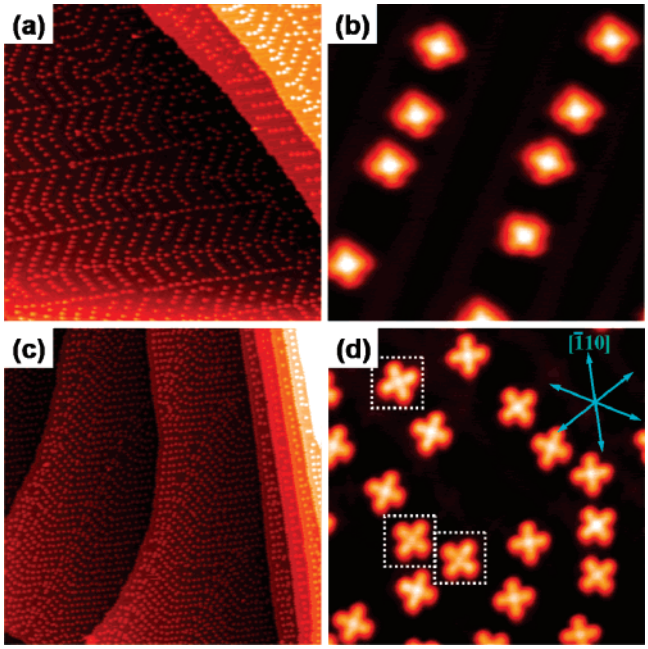

Figure 1. (a, b) STM images of ~0.1 ML FePc molecules on Au(111) surface, $V = -1.5$ V, $I = 0.05$ nA, the image sizes are (a) 150 nm × 150 nm and (b) 14 nm × 14 nm. (c, d) STM images of ~0.3 ML FePc molecules on Au(111) surface, $V = 0.5$ V, $I = 0.05$ nA, the image sizes are (c) 150 nm × 150 nm and (d) 14 nm × 14 nm. The set of three arrows in d indicates the closed-packed directions of the Au(111) substrate. Two kinds of adsorption configurations are identified according to the molecular orientation with the underlying Au(111) surface. Molecules of configuration II are marked with squares and the rest of the molecules belong to configuration I in d.

energy for the plane waves was 400 eV. All parameters were well tested to ensure a total energy convergence of about 1 meV per atom. In structural relaxations, all atoms except for the bottom two Au layers were fully relaxed until the net force on every atom was smaller than 0.02 eV/Å.

Results and Discussion

A. Low Submonolayer Coverage. The planar FePc molecule is constituted by a flat ring bonded to four benzene rings with a single iron ion in the central cavity.[28] The first STM images of FePc on Au(111) were reported by Hipps et al.[28] Figure 1a and c displays the large-scale STM images of FePc molecules on the Au(111) surface at the coverage of ~0.1 ML and ~0.3 ML, respectively, where 1 ML is defined as the amount of deposited FePc that entirely covers the substrate. Because of the sufficient suppression of thermal diffusion at 5 K, individual FePc molecules can be clearly resolved. The FePc molecules are recognized as a four-lobed "cross" structure with a protrusion at the center, which is consistent with its chemical structure, and with enhanced tunneling through the half-filled d_{z^2} orbital of Fe.[28] The size of the protrusion indicates that the FePc molecules are flat on Au(111) surface, as shown in the corresponding close-up STM images of Figure 1b and d. The effect of the herringbone reconstruction is clearly displayed by the inhomogeneous distribution of FePc molecules on the Au(111) surface. At the coverage of ~0.1 ML, most FePc molecules deposit on the fcc regions, and few molecules deposit on the elbow areas of the hcp regions. This preference indicates that the FePc molecules are more stable on fcc regions than on hcp regions. At an increased coverage of ~0.3 ML, the FePc molecules deposit on both the fcc and the hcp regions of the reconstructed Au(111) surface. The set of the three arrows in Figure 1d represents the equivalent close-packed directions of the Au(111) surface.

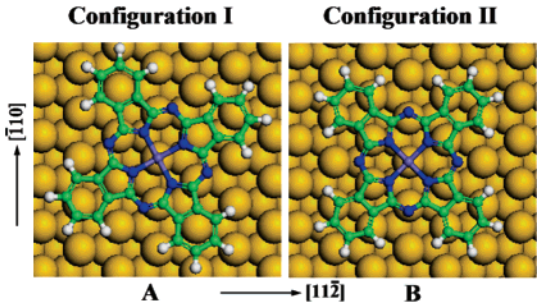

Figure 2. The precise adsorption configurations for FePc molecules on Au(111) surface at submonolayer coverage. (A) and (B) are the real space model structures for the experimentally observed configuration I and configuration II of FePc on Au(111) surface, respectively.

The common characteristic at both submonolayer coverages is that the FePc molecules prefer to deposit dispersedly as isolated adsorbates, that is, FePc molecules form neither compact aggregations nor ordered structures, which reveal the weak intermolecular interaction at low submonolayer coverages. The oriented adsorption of the flat-lying FePc molecules is also a very interesting feature. The detailed analysis of the molecular orientation with the underlying Au(111) surface reveals two molecular configurations for FePc molecules on the Au(111) surface in our STM results. For one configuration, called configuration I, the molecule cross is directed in [11$\bar{2}$] direction of the Au(111) substrate. For the other configuration, called configuration II, the cross rotates with respect to the molecular center by ~15° compared to configuration I. Because of the 3-fold symmetry of the Au(111) substrate, both configuration I and configuration II include three rotationally equivalent configurations. In Figure 1d, the molecules in configuration II are marked with dotted squares, and the rest of the molecules are in configuration I. A statistical analysis shows that approximately 80% of the FePc molecules prefer configuration I, which should be the most stable adsorption configuration. In the previous works about MPcs on Au(111) surface, only configuration I is reported. Configuration II shows a new molecular orientation, which has not been reported in previous investigations on either MPcs or their derivatives on Au(111) surface.

To identify the above precise configurations for FePc on Au(111), first-principles calculations based on DFT have been carried out. The calculation results reveal that the A and B configurations in Figure 2 are the most stable configurations with an energy difference of 91 meV, and their orientations correspond to configuration I and configuration II in the STM results, respectively. In both configuration I and II, the molecular centers are on the top site of Au(111) surface, indicating a strong interaction between iron and gold atoms.

B. High Submonolayer Coverage. Figure 3a displays a representative STM image of ~0.6 ML molecules on Au(111) surface. Although few isolated molecules can still be observed, most of the molecules are roughly arranged into linear aggregations along the domain walls. Molecular dimers, trimers, and short chains are formed on narrow hcp regions, while approximately molecular double chains are observed on wide fcc regions. The linear characteristic results from the confinement of the domain walls of Au(111) surface are similar to the CoPc molecules on Au(111) surface at submonolayer coverage.[16] Interestingly, many molecular hexamers with a central hole are observed at elbow areas of fcc regions, marked by circles in

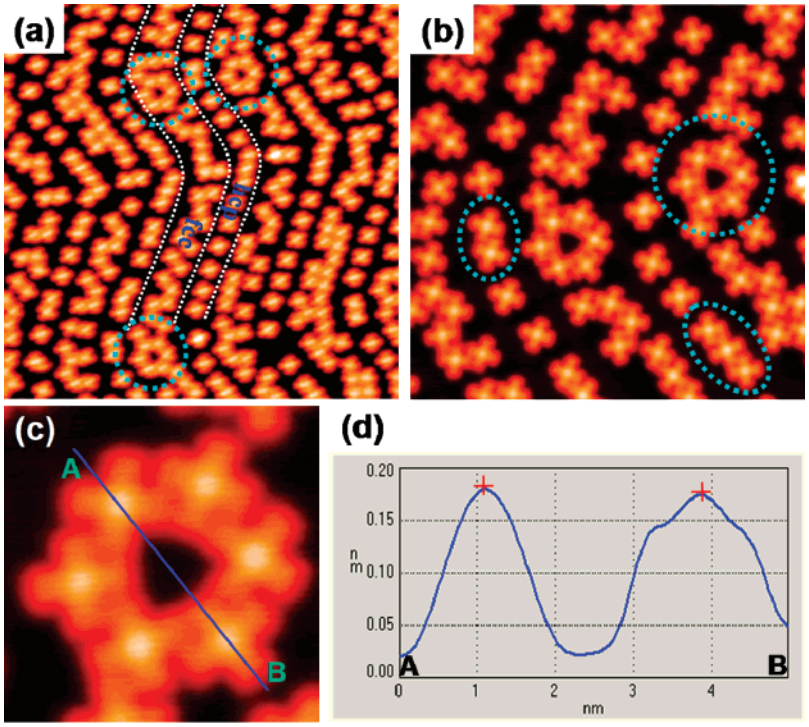

Figure 3. STM images of ~0.6 ML FePc molecules on Au(111) surface. (a) 40 nm × 40 nm, $V = -1.5$ V, $I = 0.05$ nA; (b) 20 nm × 20 nm, $V = -1.2$ V, $I = 0.05$ nA. Broken white lines indicate domain walls of the Au(111) herringbone reconstruction. Typical molecular aggregations are marked with dashed circles. (c) A close-up image of the marked hexamer in b. (d) The line profile across the hexamer along the [1$\bar{2}$1] direction from A to B in c.

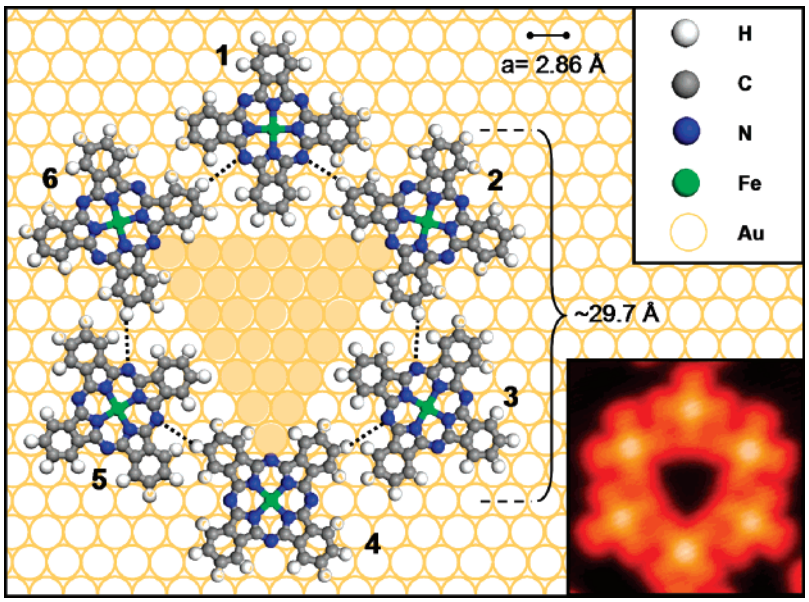

Figure 4. Model of FePc molecules forming hexamer with the underlying Au(111) substrate. The directional electrostatic interactions between the neighboring molecules are indicated by the dashed lines. Each molecule of configuration II (2, 4, and 6) connects with its neighboring molecules of configuration I (1, 3, and 5) by its two phenyl groups fitting into the hollow sites of its neighboring molecules, where the nitrogen atoms reside close to hydrogen atoms of neighboring molecules.

Figure 3a, and all the hexamers show the identical structure and orientation with the underlying Au(111) substrate. On the basis of their deposition sites on Au(111) surface, it can be concluded that the proper size of the fcc elbow areas confined by the domain walls plays an important role in the formation of the hexamers.

Three typical aggregations are marked with circles in Figure 3b. All molecules in the aggregations prefer to connect with each other by the phenyl group of one molecule fitting into the hollow site of its neighbors, indicating a directional attractive intermolecular interaction. A molecular hexamer is shown in a close-up image of Figure 3c, in which the orientations of the constituting molecules with the underlying Au(111) substrate are clearly resolved. A detailed analysis reveals that the six molecules of the hexamer adopt the six adsorption configurations (all three symmetry equivalents of configurations I and II). A line profile from A to B in Figure 3c is shown in Figure 3d, which gives a distance of ~28.5 Å between the centers of two opposite molecules. The central hole of the hexamer looks like an equilateral triangle.

A model for the hexamer is proposed in Figure 4, directly showing the molecular orientations with the underlying Au-

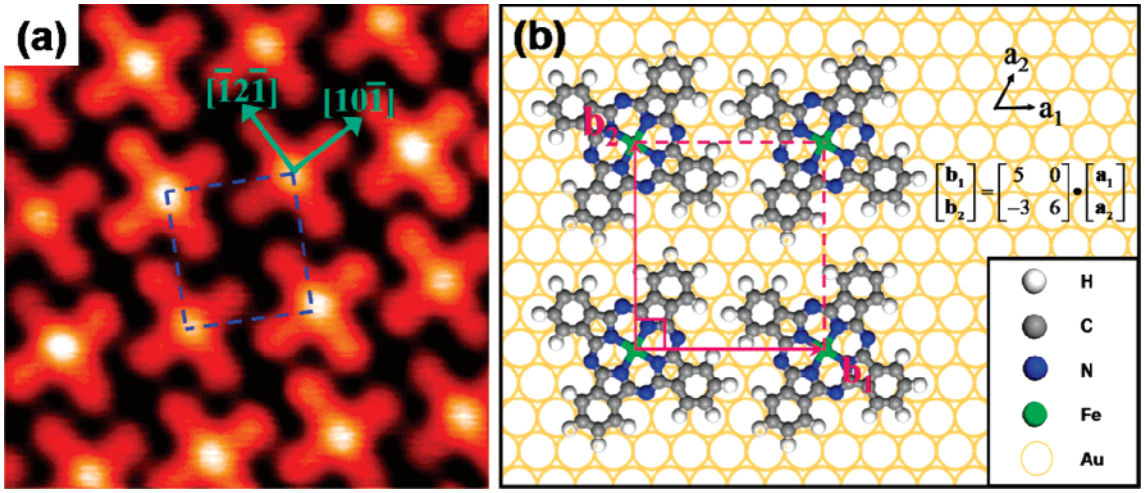

Figure 5. (a) High-resolution STM image of FePc on Au(111) surface at saturated coverage (6 nm × 6 nm, $V = -0.4$ V, $I = 0.05$ nA). Only the FePc molecules of configuration I are observed in the quasi-quadratic ordered FePc monolayer on Au(111) surface. (b) The model for one unit cell of FePc molecule monolayer on Au(111).

(111) substrate. Each molecule in configuration II (2, 4, and 6) connects with its neighboring molecules in configuration I (1, 3, and 5) by its two phenyl groups fitting into the hollow sites of its neighboring molecules, where the nitrogen atoms reside close to hydrogen atoms of neighboring molecules. The electrostatic interaction between the unshared electron pair of the nitrogen atom and the net positive hydrogen atom of the phenyl group of the neighboring molecule is the origin of the directional attractive interaction between molecules. In the model of Figure 4, the distance between the centers of molecules 1 and 4 in the proposed model accounts to 29.7 Å, which is in agreement with the experimental value in the line profile of Figure 3d. The central triangle dark area in the model is also consistent with the central hole of the molecular hexamer in STM image. On the basis of the above analysis, it is apparent that the formation of the peculiar porous hexamer structure reveals the effect of both the specific adsorption configurations determined from the molecule−substrate interaction and the directional attractive intermolecular interaction as well as the effect of the herringbone reconstruction.

C. Monolayer Coverage. At the saturated coverage, FePc molecules form an almost perfectly ordered layer.[28] A close-up STM image of Figure 5a shows the distinctive four-lobed shape of the FePc molecules and their assembling with quasi-quadratic unit cell on the FePc monolayer. One unit cell is marked with dashed lines in Figure 5a. All the molecules of the monolayer prefer configuration I, in contrast to the two configurations at the submonolayer coverage. It can be concluded that directional intermolecular interactions became more important than the molecule−substrate interactions as the coverage increased. As a result, all the FePc molecules deposit on Au(111) surface only in the most stable configuration, configuration I. A molecular model of the quasi-quadratic unit cell is given in Figure 5b, where the molecular orientation and the commensurate superstructure of the FePc monolayer are clearly displayed.

Conclusions

We have investigated the configurations and growth behavior of FePc on Au(111) surface by means of low-temperature STM and DFT calculations. The growth behavior of FePc on Au(111) represents a coverage-dependent competition between molecule−substrate and the laterally intermolecular interactions. At low coverages, FePc molecules prefer to adsorb on terrace dispersedly as isolated adsorbates because of the weak molecule−molecule interactions. At high surface coverages, the FePc molecules assemble to form dimers, trimers, and short chains and even peculiar porous hexamers. The characteristic development is caused by directional lateral interactions between neighboring FePc molecules at the decreased intermolecular distances at high coverages. Two different adsorption configurations (I and II) for FePc on Au(111) surface at submonolayer coverage are resolved on the basis of STM image analysis and DFT calculations, which are determined by the strong molecule−substrate interaction. At the saturated coverage, highly ordered FePc monolayer with only configuration I is observed because of the stronger interactions between molecules than that between molecule and substrate. This investigation is helpful for a deep and comprehensive understanding on the adsorption and growth behavior of FePc and other MPc molecules on Au(111) at the submonolayer coverage.

Acknowledgment. This project is supported partially by the Natural Science Foundation of China (NSFC), (Grant No. 90406022), National 973 and 863 projects of China.

References and Notes

(1) Crone, B.; Dodabalapur, A.; Lin, Y.-Y.; Filas, R. W.; Bao, Z.; LaDuca, A.; Sarpeshkar, R.; Katz, H. E.; Li, W. *Nature* (London) **2000**, *403*, 521.

(2) Dimitrakopoulos, C. D.; Malenfant, P. R. L. *Adv. Mater.* **2002**, *14*, 99.

(3) Witte, G.; Wöll, C. *J. Mater. Res.* **2004**, *19*, 1889.

(4) Horowitz, G. *J. Mater. Res.* **2004**, *19*, 1946.

(5) Gao, H.-J.; Sohlberg, K.; Xue, Z. Q.; Chen, H. Y.; Hou, S. M.; Ma, L. P.; Fang, X. W.; Pang, S. J.; Pennycook, S. J. *Phys. Rev. Lett.* **2000**, *84*, 1780. Ma, L. P.; Song, Y. L.; Gao, H.-J.; Zhao, W. B.; Chen H. Y.; Xue, Z. Q.; Pang, S. J. *Appl. Phys. Lett.* **1996**, *69*, 3752. Gao, H.-J.; Xue, Z. Q.; Wang, K. Z.; Wu, Q. D.; Pang, S. J. *Appl. Phys. Lett.* **1996**, *68*, 2192. Gao, H.-J.; Ma, L. P.; Zhang, H. X.; Chen, H. Y.; Xue, Z. Q.; Pang, S. J. *J. Vac. Sci. Technol., B* **1997**, *15*, 1581. Gao, H.-J.; Wang, D. W.; Liu, N.; Xue, Z. Q.; Pang, S. J. *J. Vac. Sci. Technol., B* **1996**, *14*, 1349.

(6) Barlow, S. M.; Raval, R. *Surf. Sci. Rep.* **2003**, *50*, 201.

(7) Eremtchenko, M.; Schaefer, J. A.; Tautz, F. S. *Nature* (London) **2003**, *425*, 602.

(8) Forrest, S. R. *Chem. Rev.* **1997**, *97*, 1793.

(9) Theobald, J. A.; Oxtoby, N. S.; Phillips, M. A.; Champness, N. R.; Beton, P. H. *Nature* (London) **2003**, *424*, 1029.

(10) Böhringer, M.; Morgenstern, K.; Schneider, W. D.; Berndt, R.; Mauri, F.; De Vita, A.; Car, R. *Phys. Rev. Lett.* **1999**, *83*, 324.

(11) Barth, J. V.; Weckesser, J.; Cai, C.; Günter, P.; Bürgi, L.; Jeandupeux, O.; Kern, K. *Angew. Chem., Int. Ed.* **2000**, *39*, 120.

(12) Lukas, S.; Witte, G.; Wöll, Ch. *Phys. Rev. Lett.* **2002**, *88*, 028301.

(13) Gao, L.; Deng, Z. T.; Ji, W.; Lin, X.; Cheng, Z. H.; He, X. B.; Shi, D. X.; Gao, H.-J. *Phys. Rev. B* **2006**, *73*, 075424. Du, S. X.; Gao, H. -J.;

Seidel, C.; Tsetseris, L.; Ji, W.; Kopf, H.; Chi, L. F.; Fuchs, H.; Pennycook, S. J.; Pantelides, S. T. *Phys. Rev. Lett.* **2006**, *97*, 156105.

(14) Wang, Y. L.; Ji, W.; Shi, D. X.; Du, S. X.; Seidel, C.; Ma, Y. G.; Gao, H.-J.; Chi, L. F.; Fuchs, H. *Phy. Rev. B* **2004**, *69*, 075408. Shi, D. X.; Ji, W.; Lin, X.; He, X. B.; Lian, J. C.; Gao, L.; Cai, J. M.; Lin, H.; Du, S. X.; Lin, F.; Seidel, C.; Chi, L. F.; Hofer, W. A.; Fuchs, H.; Gao, H.-J. *Phys. Rev. Lett.* **2006**, *96*, 226101.

(15) Seidel, C.; Poppensieker, J.; Fuchs, H. *Surf. Sci.* **1998**, *408*, 223.

(16) Barlow, D. E.; Scudiero, L.; Hipps, K. W. *Langmuir* **2004**, *20*, 4413.

(17) Gomer, R. *Rep. Prog. Phys.* **1990**, *53*, 917.

(18) Venables, J. A. *Introduction to Surface and Thin Film Processes*; Cambridge University Press: Cambridge, U.K., 2000.

(19) Brune, H. *Surf. Sci. Rep.* **1998**, *31*, 121.

(20) Barth, J. V. *Surf. Sci. Rep.* **2000**, *40*, 75.

(21) Yokoyama, T.; Yokoyama, S.; Kamikado, T.; Okuno, Y.; Mashiko, S. *Nature* (London) **2001**, *413*, 619.

(22) Barth, J. V.; Weckesser, J.; Trimarchi, G.; Vladimirova, M.; DeVita, A.; Cai, C.; Brune, H.; Günter, P.; Kern, K. *J. Am. Chem. Soc.* **2002**, *124*, 7991.

(23) Han, P.; Mantooth, B. A.; Sykes, E. C. H.; Donhauser, Z. J.; Weiss, P. S. *J. Am. Chem. Soc.* **2004**, *126*, 10787.

(24) Joachim, C.; Gimzewski, J. K.; Aviram, A. *Nature* (London) **2000**, *408*, 541.

(25) Cracium, M. F.; Rogge, S.; Morpurgo, A. F. *J. Am. Chem. Soc.* **2005**, *127*, 12210.

(26) Papageorgiou, N.; Salomon, E.; Angot, T.; Layet, J.-M.; Giovanelli, L.; Lay, G. L. *Prog. Surf. Sci.* **2004**, *77*, 139.

(27) Lu, X.; Hipps, K. W.; Wang, X. D.; Mazur, U. *J. Am. Chem. Soc.* **1996**, *118*, 7197.

(28) Hipps, K. W.; Lu, X.; Wang, X. D.; Mazur, U. *J. Phys. Chem.* **1996**, *100*, 11207.

(29) Lu, X.; Hipps, K. W. *J. Phys. Chem. B* **1997**, *101*, 5391.

(30) *J. Phys. Chem. B* **2000**, *104*, 5993.

(31) Yoshimoto, S.; Tada, A.; Suto, K.; Itaya, K. *J. Phys. Chem. B* **2003**, *107*, 5836−5843.

(32) Suto, K.; Yoshimoto, S.; Itaya, K. *J. Am. Chem. Soc.* **2003**, *125*, 14976−14977.

(33) Yoshimoto, S.; Tsutsumi, E.; Suto, K.; Honda, Y.; Itaya, K. *Chem. Phys.* **2005**, *319*, 147−158.

(34) Lackinger, M.; Hietscholda, M. *Surf. Sci.* **2002**, *520*, L619−L624.

(35) Cheng, Z. H.; Gao, L.; Deng, Z. T.; Liu, Q.; Jiang, N.; Lin, X.; He, X. B.; Du, S. X.; Gao, H.-J. *J. Phys. Chem. C* **2007**, *111*, 2656−2660.

(36) Perdew, J. P.; Chevary, J. A.; Vosko, S. H.; Jackson, K. A.; Pederson, M. R.; Singh, D. J.; Fiolhais, C. *Phys. Rev. B* **1992**, *46*, 6671.

(37) Blöchl, P. E. *Phys. Rev. B* **1994**, *50*, 17953.

(38) Kresse, G.; Joubert, D. *Phys. Rev. B* **1999**, *59*, 1758.

(39) Kresse, G.; Furthmüller, J. *Phys. Rev. B* **1996**, *54*, 11169.

(40) Kresse, G.; Hafner, J. *Phys. Rev. B* **1993**, *47*, R558.